A methodology for the design of robust rollover prevention controllers for automotive vehicles using differential braking

March 15, 2009

Abstract

In this paper we apply recent results from robust control to the problem of rollover prevention in automotive vehicles. Specifically, we exploit the results of [6] which provide controllers to robustly guarantee that the peak values of the performance outputs of an uncertain system do not exceed certain values. As a measure of performance for rollover prevention, we use the Load Transfer Ratio LTR_d introduced in [21], and design differential-braking-based rollover controllers to keep the value of this quantity below a certain level; we also obtain controllers which yield robustness to variations in vehicle speed. We present numerical simulations using a nonlinear multi-body vehicle simulation model to demonstrate the effectiveness of our controllers in preventing rollover.

Keywords: vehicle rollover, vehicle active safety, vehicle active rollover prevention, robust control.

1 Introduction

It is well known that vehicles with a high center of gravity such as vans, pickups, and the highly popular SUVs (Sport Utility Vehicles) are more prone to rollover accidents. According to the 2004 data [1], light trucks (pickups, vans and SUV's) were involved in nearly 70% of all the rollover accidents in the USA, with SUV's alone responsible for almost 35% of this total. The fact that the composition of the current automotive fleet in the U.S. consists of nearly 36% pickups, vans and SUV's [2], along with the recent increase in the popularity of SUV's worldwide, makes rollover an important safety problem.

There are two distinct types of vehicle rollover: tripped and un-tripped. A tripped rollover commonly occurs when a vehicle slides sideways and digs its tires into soft soil or strikes an object such as a curb or guardrail. Driver induced un-tripped rollover can occur during typical driving situations and poses a real threat for top-heavy vehicles. Examples are excessive speed during cornering, obstacle avoidance and severe lane change maneuvers, where rollover occurs as a direct result of the lateral wheel forces induced during these maneuvers. In recent years, rollover has been the subject of intensive research, especially by the major automobile manufacturers; see, for example, [3, 4]. That research is geared towards the development of rollover prediction schemes and occupant protection devices. It is however, possible to prevent such a rollover incident by monitoring the car dynamics and applying proper control effort ahead of time. Therefore there is a need to develop driver assistance technologies which would be transparent to the driver during normal driving conditions, while acting in emergency situations to recover handling of the vehicle until the driver recovers control of the vehicle [5].

We present in this paper a robust rollover prevention controller design methodology based on differential braking. The proposed control design is an application of recent results on the design of control systems which guarantee that the peak values of the performance outputs of a plant do not exceed certain thresholds when subject to bounded disturbance inputs [6, 7]. The main selected performance output for the rollover problem is the Load Transfer Ratio LTR_d. This measure of performance is related to tire lift-off and it can be considered as an early indicator of impending vehicle rollover. We also include the braking force as a performance output to take into account limitations on the maximum braking force. The aim of our control strategy is to maximize the magnitude of the allowable disturbance inputs which do not drive the performance outputs outside their prespecified limits; in this case the disturbance input is the driver steering input. We also want to guarantee robustness with respect to the parameter uncertainty that arises from changing vehicle speed. We indicate how our design can be extended to account for other sources of uncertainty such as unknown vehicle center of gravity and tire stiffness parameters.

2 Related work

Rollover prevention is a topical area of research in the automotive industry (see, for example, the rollover section at *http://www.safercar.gov/* for a good introduction to the problem) and several studies have recently been published. Relevant publications include that of Palkovics et al. [8], where they proposed the ROP (Roll-Over Prevention) system for use in commercial trucks making use of the wheel slip difference on the two sides of the axles to estimate the tire lift-off prior to rollover. Wielenga [9] suggested the ARB (Anti Roll Braking) system utilizing braking of the individual front wheel outside the turn or the full front axle instead of the full braking action. The suggested control system is based on lateral acceleration thresholds and/or tire lift-off sensors in the form of simple contact switches. Chen et al. [10] suggested using an estimated TTR (Time To Rollover) metric as an early indicator for the rollover threat. When TTR is less than a certain preset threshold value for the particular vehicle under interest, they utilized differential braking to prevent rollover. Ackermann et al. and Odenthal et al. [11], [12] proposed a robust active steering controller, as well as a combination of active steering and emergency braking controllers. They utilized a continuous-time active steering controller based on roll rate measurement. They also suggested the use of a static Load Transfer Ratio (LTR_s) which is based on lateral acceleration measurement; this was utilized as a criterion to activate the emergency steering and braking controllers.

3 Vehicle modeling and LTR_d

In this section we introduce the model that we use for controller design. We define the rollover detection criterion LTR_d and present the assumptions on the sensors and actuators used in the design. We also present the higher fidelity nonlinear multi-body simulation model to which the controllers will be applied.

3.1 Vehicle model for control design

We use a linearized vehicle model for control design. Specifically, we consider the well known single-track bicycle model with a roll degree of freedom as illustrated in Figure 1. In this model the steering angle δ, the roll angle ϕ and the vehicle sideslip angle β are all assumed to be small. We further assume that all the vehicle mass is sprung, which implies insignificant unsprung mass.

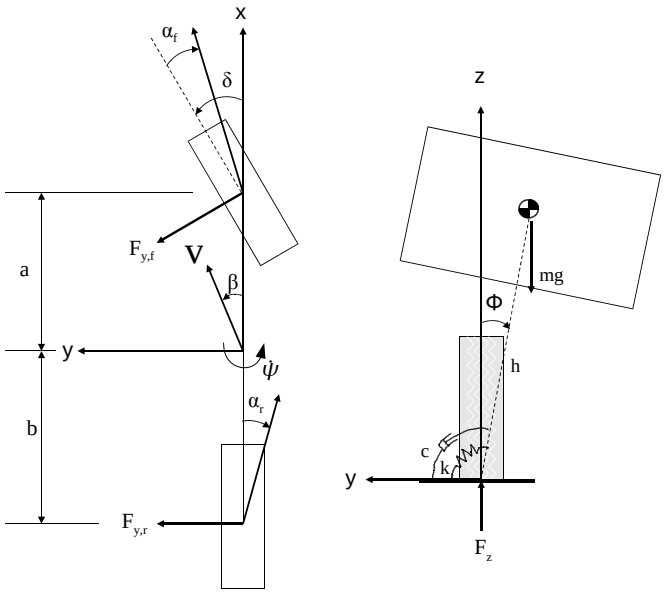

Figure 1: Linear bicycle model with roll degree of freedom.

The lateral forces on the front and rear tires, denoted by $F_{y,f}$ and $F_{y,r}$, respectively, are represented as linear

functions of the tire slip angles α_f and α_r, that is, $F_{y,f} = C_{\alpha,f}\alpha_f$ and $F_{y,r} = C_{\alpha,r}\alpha_r$, where $C_{\alpha,f}$ and $C_{\alpha,r}$ are the front and rear tire stiffness parameters, respectively. In order to simplify the model description, we further define the following auxiliary variables

$$\begin{aligned} \sigma &\triangleq C_{\alpha,f} + C_{\alpha,r} \\ \rho &\triangleq C_{\alpha,r}b - C_{\alpha,f}a \\ \kappa &\triangleq C_{\alpha,f}a^2 + C_{\alpha,r}b^2 \end{aligned} \tag{1}$$

where the lengths a and b are defined in Figure 1. For simplicity, it is assumed that, relative to the unsprung mass, the sprung mass rolls about a horizontal roll axis which is along the centerline of the unsprung mass and at ground level. Using the parallel axis theorem of mechanics, $J_{x_{eq}}$, the moment of inertia of the vehicle about the assumed roll axis, is given by

$$J_{x_{eq}} = J_{xx} + mh^2, \tag{2}$$

where h is the distance between the vehicle center of gravity (CG) and the assumed roll axis and J_{xx} is the moment of inertia of the vehicle about the roll axis through the CG. Introducing the state $x = \begin{bmatrix} \beta & \dot{\psi} & \dot{\phi} & \phi \end{bmatrix}^T$, where $\dot{\psi}$ is the yaw rate of the unsprung mass, the motion of this model can be described by

$$\dot{x} = Ax + B_{\delta_s}\delta_s + B_u u \tag{3}$$

where

$$\begin{aligned} A &= \begin{bmatrix} -\frac{\sigma J_{xeq}}{mJ_{xx}v} & \frac{\rho J_{xeq}}{mJ_{xx}v^2} - 1 & -\frac{hc}{J_{xx}v} & \frac{h(mgh-k)}{J_{xx}v} \\ \frac{\rho}{J_{zz}} & -\frac{\kappa}{J_{zz}v} & 0 & 0 \\ -\frac{h\sigma}{J_{xx}} & \frac{h\rho}{J_{xx}v} & -\frac{c}{J_{xx}} & \frac{mgh-k}{J_{xx}} \\ 0 & 0 & 1 & 0 \end{bmatrix}, \\ B_{\delta_s} &= \frac{\pi}{180\lambda_s}\begin{bmatrix} \frac{C_{\alpha,f}J_{xeq}}{mJ_{xx}v} & \frac{C_{\alpha,f}a}{J_{zz}} & \frac{hC_{\alpha,f}}{J_{xx}} & 0 \end{bmatrix}^T, \\ B_u &= \begin{bmatrix} 0 & -\frac{T}{2J_{zz}} & 0 & 0 \end{bmatrix}^T \end{aligned} \tag{4}$$

where the steering wheel angle δ_s is the steering input applied to the steering wheel (in degrees) and λ_s is the steering ratio between the steering wheel input and the steering angle δ of the front wheels.

Control input u represents the differential braking force on the wheels; it is positive if braking is on the right wheels and negative if braking is on the left wheels. Note that we can brake either front, rear or both of the wheels on each side of the vehicle depending on the maneuver and u is the total effective braking force acting on either side.

Further definitions for all the parameters in (4) are given in Table 1. See [13] for a detailed derivation of this vehicle model.

3.2 The Load Transfer Ratio, LTR_d

Traditionally, as discussed in the related work section, some estimate of the vehicle load transfer ratio (LTR) has been used as a basis for the design of rollover prevention systems. The quantity LTR [12, 14] can be simply defined as the load (i.e., vertical force) difference between the left and right wheels of the vehicle, normalized by the total load; these forces are illustrated in Figure 2. In other words

$$LTR = \frac{\text{Load on Right Tires-Load on Left Tires}}{\text{Total Load}}. \tag{5}$$

Clearly, LTR varies within $[-1, 1]$, and for a perfectly symmetric car that is driving straight, it is zero. The extrema are reached in the case of a wheel lift-off of one side of the vehicle, in which case LTR becomes 1 or -1 depending on the side that lifts off. If roll dynamics are ignored, it is easily shown [12] that the corresponding LTR (which we denote by LTR_s) is approximated by

$$LTR_s \triangleq \frac{2a_y h}{gT}, \tag{6}$$

Table 1: Model parameters and their definitions

Parameter	Description	Unit
m	vehicle mass	$[kg]$
v	vehicle speed	$[m/s]$
J_{xx}	roll moment of inertia at CG	$[kg \cdot m^2]$
J_{zz}	yaw moment of inertia at CG	$[kg \cdot m^2]$
a	longitudinal CG position w.r.t. front axle	$[m]$
b	longitudinal CG position w.r.t. rear axle	$[m]$
T	vehicle track width	$[m]$
h	distance of CG from roll axis	$[m]$
c	suspension damping coefficient	$[N \cdot m \cdot s/rad]$
k	suspension spring stiffness	$[N \cdot m/rad]$
$C_{\alpha,f}$	linear tire stiffness for front tire	$[N/rad]$
$C_{\alpha,r}$	linear tire stiffness for rear tire	$[N/rad]$
δ	steering angle	$[deg]$
δ_s	steering wheel angle	$[deg]$
λ_s	steering ratio	

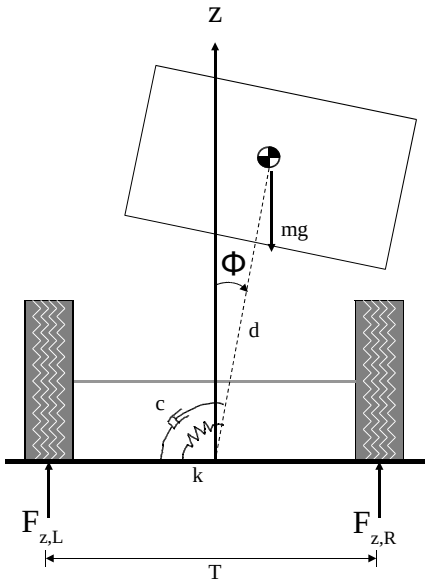

Figure 2: Combined vertical forces for each side of vehicle

where a_y is the lateral acceleration of the CG.

The rollover estimation based upon (6) is not sufficient to detect the transient phase of rollover (due to the fact that it is derived ignoring roll dynamics.) Consequently, we follow [21] and obtain an expression for LTR which does not ignore roll dynamics. We denote this by LTR_d. In order to derive LTR_d we write a torque balance equation. Recall that we assumed the unsprung mass is insignificant and the main body of the vehicle rolls about an axis along the centerline of the unsprung mass at the ground level. We can write a torque balance for the unsprung mass about the assumed roll axis in terms of the suspension torques and the vertical wheel forces as follows:

$$-F_{z,R}\frac{T}{2} + F_{z,L}\frac{T}{2} - k\phi - c\dot{\phi} = 0\,. \tag{7}$$

Now substituting the definition of LTR from (5) and approximating the total load by the vehicle weight, yields the following expression for LTR_d:

$$LTR_d \quad = \quad -\frac{2(c\dot{\phi}+k\phi)}{mgT}. \tag{8}$$

In terms of the state x, LTR_d can be described by

$$LTR_d = C_1 x, \tag{9}$$

where

$$C_1 = \left[\begin{array}{cccc} 0 & 0 & -\frac{2c}{mgT} & -\frac{2k}{mgT} \end{array} \right]. \tag{10}$$

3.3 Actuators, sensors and parameters

We are interested in control design based on differential braking. Active braking actuators are already available in many modern production cars that are equipped with systems such as ABS (Anti-lock Braking System) and EBS (Electronic Brake System) or similar systems, which are capable of selectively braking each of the wheels. The fact that control designs using these actuators can be commissioned without much financial overhead makes them the preferred actuator candidates in the literature.

We also assume full state feedback information for the design of the controllers and that all the model parameters are known. This is an unrealistic assumption; however, our control design is easily extended to account for uncertainty in these parameters. As a side note, although we assumed all the vehicle model parameters to be known, it is possible to estimate some of these that are fixed (but unknown) using the sensor information available for the control design suggested here; this however is outside the scope of this work [15].

3.4 A high-fidelity nonlinear simulation model

Although we base control design on the linear bicycle model, controller evaluation is carried out on a higher fidelity nonlinear simulation model of a vehicle which we call the SimMechanics Vehicle Simulation Model (SM). This model is created using the multi-body simulation package SimMechanics which is integrated into Mathworks's Matlab/Simulink. This is convenient for using various analysis tools in Matlab.

In general, a Simechanics model consists of bodies connected together by various joints and subject to various forces. Our SM model consists of six unsprung bodies (four wheels and two axles) of negligible mass and one sprung body as shown in Figure 3. Between the sprung mass and each of the axles, there is a joint which permits a roll degree-of-freedom (DOF); the location of these two joints defines the body roll axis. At each of these roll joints there is a torsional spring and damper between the sprung mass and the corresponding axle; this models the vehicle suspension. Connected to each axle are left and right wheels, with the front wheels having a yaw DOF relative to the front axle to allow for a steering angle, whereas the rear wheels are rigidly fixed to the rear axles. Each wheel has a contact point where longitudinal, lateral and vertical tire forces are applied. These contact points can leave the ground allowing the vehicle to roll over. This is a nonlinear model in which any or all wheels can leave the ground and can be used to simulate rollover.

The tire force model used here is based on the Magic Formula model developed by Pacekja [16]. This model captures the nonlinear characteristics of the tire forces at large sideslip angles and the effect of the vertical tire force F_z on the lateral tire force F_y; see Figure 4 for an definition of the tire force components. With zero longitudinal force F_x, the vertical force depends on the vehicle loading and motion. the lateral force is a function of the vertical force, the tire slip angle α, tire lateral stiffness and the friction coefficient between the tire and ground, as described by the Magic Formula model [16]. Figure 5 shows the lateral force as a function of slip angle for various vertical forces (with fixed tire stiffness and friction coeffcient), demonstrating the non-linearity of the Magic Formula function. Note that the peak lateral force and the saturation slip angle are functions of the vertical force.

The introduction of a longitudinal force F_x acting on the tire due to braking and acceleration makes it necessary to consider the limitations of the combination of lateral and longitudinal forces acting on the tire at the same time. The physical limitation on the forces applied to the tire are determined by the ground/tire longitudinal and lateral friction coefficients μ_x and μ_y, resulting in a friction ellipse of longitudinal and lateral forces. In the case where the

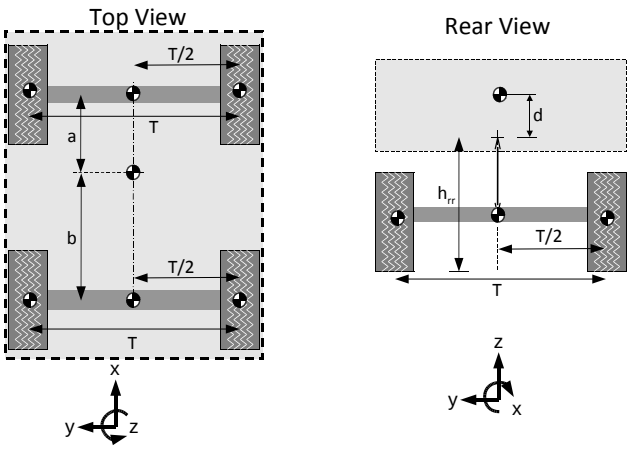

Figure 3: SimMechanics vehicle model layout

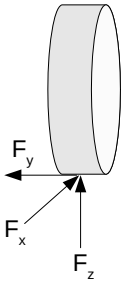

Figure 4: Tire force components

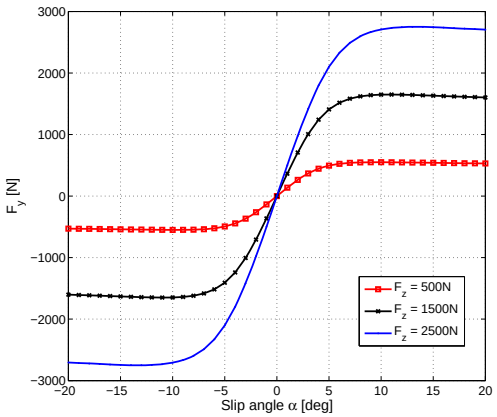

Figure 5: Lateral force as a function of the slip angle for various vertical loads

longitudinal and lateral friction coefficients are equal ($\mu_x = \mu_y = \mu$), the friction limit results in a friction circle which bounds the available lateral and longitudinal forces:

Table 2: Model parameters

parameter	value	unit
m	2800	$[kg]$
J_{xx}	2275	$[kg \cdot m^2]$
J_{zz}	16088	$[kg \cdot m^2]$
a	1.58	$[m]$
b	1.97	$[m]$
T	1.6252	$[m]$
h	0.79	$[m]$
c	12160	$[N \cdot m \cdot s/rad]$
k	221060	$[N \cdot m/rad]$
$C_{\alpha,f}$	153540	$[N/rad]$
$C_{\alpha,r}$	123650	$[N/rad]$
λ_s	18	

$$F_x^2 + F_y^2 \leq \mu^2 F_z^2 \tag{11}$$

Our model takes this constraint into account. The effects of camber on the tire result in an equivalent slip angle (α_{eq}) instead of the true tire slip angle (α), reducing the lateral forces that can be generated by the tire. These corrections need to be taken into consideration as the tire camber varies as with the wheel roll angle during rollover events.

The linear tire lateral stiffnesses used in the bicycle model are equivalent to the 'effective axle cornering stiffness' of the SM model defined by Pacejka [16]. The effective axle stiffnesses are defined as the ratio of the lateral force to virtual slip angle for each axle *i* in a steady state turn, where *i* is either the front or rear axle.

$$C_{\alpha,i} = \frac{F_{y,i}}{\alpha_{a,i}}. \tag{12}$$

To ensure that the linear tire characteristics are captured, the effective axle stiffnesses have to be calculated from the SM model in a steady state turn at low speeds to ensure that linear characteristics are captured.

Since the SM model is sprung at both front and rear axles, the overall suspension roll stiffness and damping is split between front and rear by the roll stiffness ratio KF and the roll damping ratios CF. This distribution highly affects the handling behavior of the vehicle from understeer to oversteer. In order to achieve maximum cornering ability by reducing understeer without inducing oversteer (and thus maximizing rollover propensity), the stiffness and damping ratios are set to 60% front bias.

Furthermore the limitations of the friction circle on the tire forces necessitates the use of a brake bias between front and rear braking forces to minimize the case of wheel lockup without utilizing the maximum braking force available. Although longitudinal load transfer during braking would vary the sizes of the friction circles, we consider the case of a static brake bias tuned to achieve maximum braking force initially for a range of constant lateral accelerations, and this is set to 55% front bias.

3.5 Simulation of the SM model

For comparison purposes, the sprung mass of the SM model is set equal to that of the bicycle model, while the unsprung masses set are very small; they are non-zero to prevent numerical singularities in the simulation. Furthermore, the bicycle model assumes that the roll center is on the ground plane, thus the roll center height of the SM model is set to be on the ground. The primary set of simulation parameter values used are as defined in Table 2, as obtained from [18] and [19], with parameters representative of a typical commercial van.

The vehicle is subjected to an 'elk-test' maneuver with steering wheel input profile as illustrated in Figure 6. The simulated 'elk-test' response of the linear bicycle model is compared with the response of both the nonlinear SM model and a linearization of the SM model generated via MATLAB's model linearization command 'linearize.m'.

At a speed of 20 m/s (72 kph) with a peak steering wheel angle of $\delta_{s,\max} = 60$ deg, Figure 7 demonstrates that the linearized dynamics of the SM model agree that of the bicycle model. However this also demonstrates the limitation of the linear bicycle model as a tool for prediction of rollover as it does not consider the saturation of lateral tire forces. As the maximum steering input is increased to $\delta_{s,\max} = 80$ deg (Figure 8) the differences between the linear bicycle model and the nonlinear SM model becomes even more apparent. The nonlinear SM model exhibits a significantly lower peak LTR compared to the linear models when large steering inputs are applied or when the initial velocity of the vehicle is large.

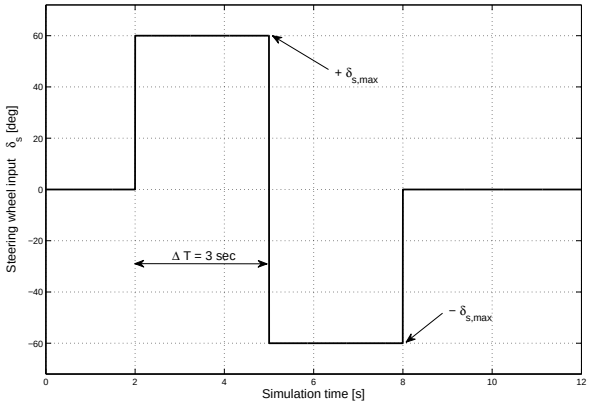

Figure 6: Steering wheel input history for simulated 'Elk-Test'

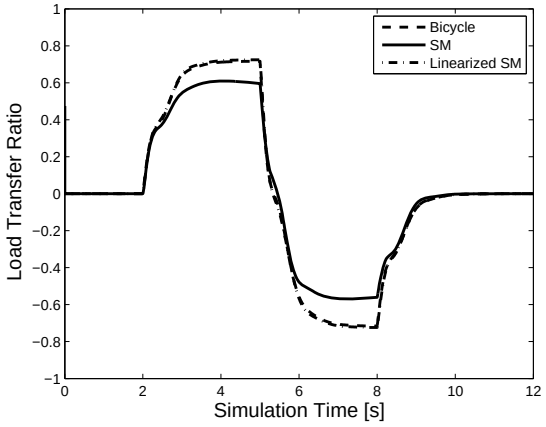

Figure 7: LTR comparison for bicycle, SM and linearized SM models at v=20 m/s and $\delta_{s,\max}$=60 deg

Further simulations with the SM model show that with large steering inputs and speeds the vehicle does roll over, which confirms the necessity for control systems to prevent such phenomenon. The SM model can be used to determine the conditions of steering input and speed which result in untripped rollover for a vehicle with parameters given in Table 2. One of the distinctions that the SM model is able to provide over the linear bicycle model is that wheel liftoff and rollover are not equivalent. In Table 3 the vehicle is tested at initial longitudinal velocities of 20, 30 and 40m/s. The steering input to lift a single wheel off the ground is denoted by $\delta_{s,lift}$, whereas the input to drive the magnitude of LTR_d to one is given by $\delta_{s,maxLTR}$. The third column of results shows $\delta_{s,roll}$, or the steering input needed to induce untripped rollover.

Full details of the SimMechanics vehicle simulation model development and verification can be found in [17].

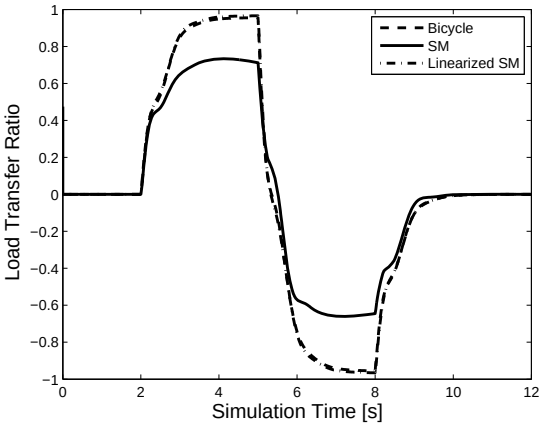

Figure 8: LTR comparison for bicycle, SM and linearized SM models at v=20 m/s and $\delta_{s,\max}$=80 deg

Table 3: Conditions for wheel lift, $|LTR_d|$ = 1 and vehicle rollover

Speed v [m/s]	$\delta_{s,lift}$ [deg]	$\delta_{s,maxLTR}$ [deg]	$\delta_{s,roll}$ [deg]
20	137	147	167
30	67	72	80
40	45	49	52

4 State feedback controllers for robust disturbance attenuation

We are interested in designing a controller to prevent rollover that is robust with respect to parameter uncertainty. Our starting point is in results obtained by Pancake, Corless and Brockman [6] for uncertain systems of the form

$$\dot{x} = A(\theta)x + B(\theta)w + B_u(\theta)u \tag{13}$$
$$z_i = C_i(\theta)x + D_{iu}(\theta)u, \qquad i = 1,\ldots,r \tag{14}$$

where $x(t) \in \mathbb{R}^n$ is the state at time $t \in [0,\infty)$, $w(t) \in \mathbb{R}^m$ is a bounded disturbance input, $u(t) \in \mathbb{R}^{m_u}$ is the control input, and $z_i(t) \in \mathbb{R}^{p_i}$, $i = 1,2,...,r$ are performance outputs. All the uncertainty and nonlinearities in the system are captured in the parameter vector θ which can depend on t, x, w and u. We wish to synthesize a stabilizing controller which prevents the peak values of the performance outputs exceeding certain values. In other words, we want to design a feedback controller, which guarantees a bounded performance output given a bounded uncertain disturbance, that is, $||w(t)|| \leq w_{max}$. We consider linear state feedback controllers of the form

$$u = Kx, \tag{15}$$

where K is a constant state feedback gain matrix. This results in a closed loop system described by

$$\dot{x} = [A(\theta) + B_u(\theta)K]x + B(\theta)w \tag{16}$$
$$z_i = [C_i(\theta) + D_{iu}(\theta)K]x, \qquad i = 1,\ldots,r. \tag{17}$$

We require the following assumptions.

Assumption 1 *There are matrices*

$$A_j,\ B_j,\ B_{uj}, \qquad j = 1,\ldots,N$$

so that for each θ, the matrix $[A(\theta)\ B(\theta)\ B_u(\theta)]$ can be written as a convex combination of $[A_1\ B_1\ B_{u1}]$,..., $[A_N\ B_N\ B_{uN}]$.

Assumption 2 *For each $i = i,\ldots,r$, there are matrices*

$$C_{ik},\ D_{iuk}, \qquad k = 1,\ldots,M_i$$

so that for each θ, the matrix $[C_i(\theta)\ D_{iu}(\theta)]$ can be written as a convex combination of $[C_{i1}\ D_{iu1}],\ldots,[C_{iM_i}\ D_{iuM_i}]$.

Remark 1 *Suppose that each of the matrices $A(\theta), B(\theta), B_u(\theta)$ depends in a multi-affine fashion on the components of an $\bar{L}$-vector θ and each element of θ is bounded; specifically,*

$$\underline{\theta}_l \le \theta_l \le \overline{\theta}_l \qquad for \qquad l = 1,\ldots,\bar{L}. \tag{18}$$

Then, for all θ, the matrix $[A(\theta)\ B(\theta)\ B_u(\theta)]$ can be expressed as a convex combination of the $2^{\bar{L}}$ vertex matrices corresponding to the extreme values of the components of θ, that is, $\theta_l = \underline{\theta}_l$ or $\overline{\theta}_l$ for $l = 1,\ldots,\bar{L}$.

We have now the following result which is useful for control design.

Theorem 1 *Consider a nonlinear/uncertain system described by (13)-(14) and satisfying Assumptions 1 and 2. Suppose that there exist matrices $S = S^T > 0$ and L along with scalars $\alpha_1,\ldots,\alpha_N > 0$ and $\gamma_1,\ldots,\gamma_r \ge 0$ such that the following matrix inequalities hold:*

$$\begin{bmatrix} A_jS + B_{uj}L + SA_j^T + L^TB_{uj}^T + \alpha_jS & B_j \\ B_j^T & -\alpha_jI \end{bmatrix} \le 0, \tag{19}$$

for $j = 1,\ldots,N$ and

$$\begin{bmatrix} -S & SC_{ik}^T + L^TD_{iuk}^T \\ C_{ik}S + D_{iuk}L & -\gamma_i^2 I \end{bmatrix} \le 0, \tag{20}$$

for $i = 1,\ldots,r$ and $k = 1,\ldots,M_i$. Then the controller

$$u = Kx \qquad with \qquad K = LS^{-1} \tag{21}$$

results in a closed loop nonlinear/uncertain system which has the following properties.

(a) The undisturbed system ($w = 0$) is globally exponentially stable, that is, all state trajectories decay exponentially.

(b) If the disturbance input is bounded, that is, $\|w(t)\| \le w_{max}$ for all t then, for zero initial state, the performance outputs $z_1,\ldots,z_r$ of the closed loop system are bounded and satisfy

$$\|z_i(t)\| \le \gamma_i w_{max}\,. \tag{22}$$

The scalars $\gamma_1,\ldots,\gamma_r$ are called *performance levels* and can be regarded as measures of the ability of the closed loop system to attenuate the effect of the disturbance input on the performance outputs; a smaller γ_i means better performance in the sense of increased attenuation. For a proof of the theorem, see [7].

5 Rollover prevention controllers and simulation results

Here we use the results of the previous section to obtain rollover prevention controllers using differential braking as the control input. We consider the steering wheel angle δ_s (in degrees) as the disturbance input.

For reasons discussed earlier, we choose $z_1 = LTR_d$ given by (8) as one performance output; we want to keep $\|z_1\| \le 1$ for the largest possible steering inputs. We consider the magnitude of the braking force u to be limited by the weight mg of the vehicle; so we choose $z_2 = u$ as a second performance output. The resulting system with two performance outputs can be described by

$$\begin{aligned} \dot{x} &= Ax + B_{\delta_s}\delta_s + B_u u \\ z_1 &= C_1 x \\ z_2 &= u\,, \end{aligned} \tag{23}$$

First we obtain a control design which is based on the above model with a fixed speed using the vehicle parameters in Table 2; we call this the fixed model controller. We then consider the effect of varying speed in our control design and we obtain a control design assuming that the speed varies over some prespecified range; we call this the robust controller.

5.1 Controller based on fixed speed

Here we base controller design on model (23) in which all matrices are constant and correspond to a fixed vehicle speed of $v = 40m/s$. To obtain a state feedback controller, we applied Theorem 1. Since we desire that $\|z_1\| \leq 1$ and $\|z_2\| \leq mg$ for the largest possible steering inputs, we considered $\gamma_2 = mg\gamma_1$. By performing a line search with respect to the scalar α we obtained a minimum value of 0.0096 for γ_1. The corresponding control gain matrix is

$$K_{uconst} = mg \cdot [\ -12.7651 \quad 5.1246 \quad 0.0854 \quad -3.6968\ ].$$

Remark 2 Consider the constant speed linear bicycle model subject to the above control gain matrix. According to (22), the constraints on the outputs will not be violated for this constant speed closed loop system if the maximum magnitude $\delta_{s,\max}$ of the steering wheel disturbance input satisfies $\delta_{s,\max} \leq 1/\gamma_1 \approx 104.69^\circ$. However application of steering inputs and the braking controller both reduce vehicle speed in the SM model. As the vehicle speed reduces, its tendency to rollover decreases and the vehicle can actually tolerate disturbance inputs with magnitude considerably larger than $1/\gamma_1$. In addition, as a consequence of the friction circle, application of braking forces reduces the maximum allowable lateral force at each wheel. In numerical simulations the above controller gain matrix was able to maintain $|LTR_d| \leq 1$ for steering input magnitudes up to $\delta_{s,\max} = 165^\circ$. However it is necessary to note that with the SM model the condition of $|LTR_d| = 1$ does not correspond to the limit for rollover, only the condition that both inside wheels lift off the ground.

For numerical simulations we chose a driver steering input corresponding to an 'elk-test' (Figure 6); we chose an initial speed of $v = 40m/s$ and first simulate the system with a steering input $\delta_{s,\max} = 35$ deg, below the liftoff requirement as stated in Table 3. The LTR response of both the controlled and uncontrolled cases are shown in Figure 9. Although the design intention of the controller is to prevent rollover, it also reduces the load transfer ratio of the vehicle significantly.

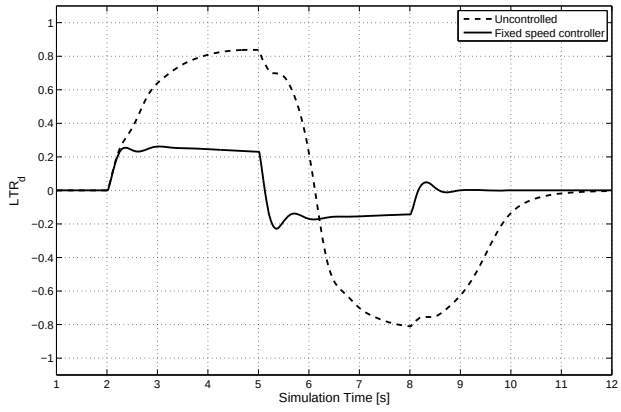

Figure 9: LTR_d response for controlled and uncontrolled vehicle simulated at below liftoff conditions.

Next we simulate the vehicle subject to an 'elk-test' maneuver with a peak steering magnitude of $\delta_{s,\max} = 104.69^\circ$. The vehicle with the proposed controller satisfies $|LTR_d| < 1$, achieving the intended design goal whereas the uncontrolled vehicle rolls over by $t = 4sec$.The corresponding normalized control history u/mg for the controller is shown in Figure 11, where we observe that the maximum input magnitude during the maneuver was 80% of the weight of the vehicle. The speed history of the vehicle is shown in Figure 11. Notice that the dramatic speed drop of the controlled vehicle is a combination of both steering inputs and braking action, suggesting there may be potential performance gains if the controller design takes into account the deceleration of the vehicle.

In the following subsection we demonstrate how our control design method can be extended to account for varying parameter uncertainties such as a variable velocity.

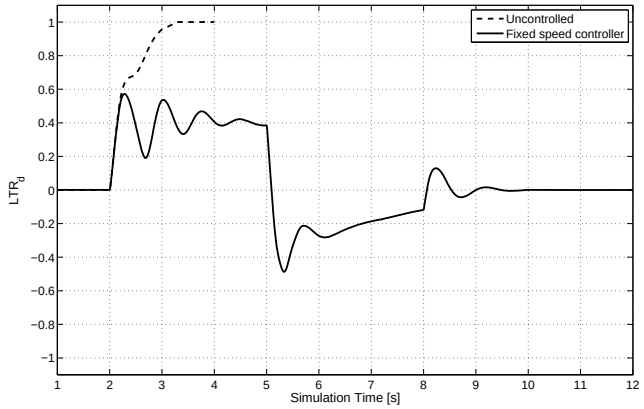

Figure 10: LTR_d response for controlled and uncontrolled vehicle

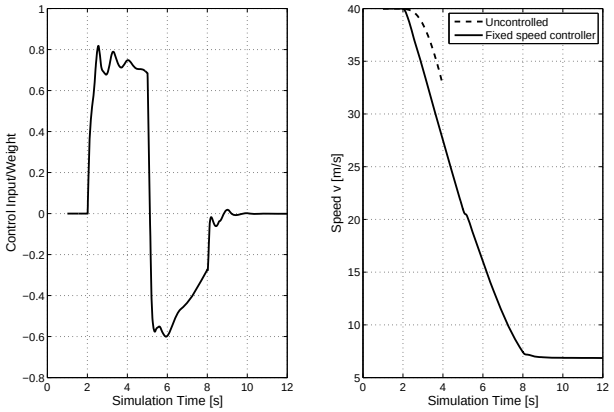

Figure 11: Normalized control history and speed history

5.2 Controller based on variable speed model

In this section, we present a rollover controller design which takes into account varying vehicle speed; we use the constant model parameters given in Table 2. We assume that the speed is bounded above and below by $\overline{v}$ and $\underline{v}$, respectively, that is, $\underline{v} \leq v \leq \overline{v}$. In order to represent typical freeway driving conditions for a compact passenger vehicle we chose $\underline{v} = 25m/s$, and $\overline{v} = 40m/s$ as the extremum design speeds. Again, we used the model (23) for controller design, where the matrices A, B_{δ_s}, B_u and C_1 are given in (4) and (10). System matrices B_u and C_1 are independent of speed. The matrices A and B_{δ_s} can be expressed as affine linear functions of the time-varying parameters $\theta_1 := 1/v$ and $\theta_2 := 1/v^2$. These parameters are bounded as follows:

$$\underline{\theta}_1 \leq \theta_1 \leq \overline{\theta}_1\,, \qquad \underline{\theta}_2 \leq \theta_2 \leq \overline{\theta}_2 \tag{24}$$

where

$$\underline{\theta}_1 = \frac{1}{\overline{v}}\,, \quad \overline{\theta}_1 = \frac{1}{\underline{v}}\,, \quad \underline{\theta}_2 = \frac{1}{\overline{v}^2}\,, \quad \overline{\theta}_2 = \frac{1}{\underline{v}^2}\,.$$

Hence our system description satisfies Assumptions 1 and 2 with the following vertex matrices

$$\begin{aligned}
A_1 &= \overline{\theta}_1 Y_1 + \overline{\theta}_2 Y_2 + Y_3\,, \qquad A_2 = \overline{\theta}_1 Y_1 + \underline{\theta}_2 Y_2 + Y_3\,,\\
A_3 &= \underline{\theta}_1 Y_1 + \overline{\theta}_2 Y_2 + Y_3\,, \qquad A_4 = \underline{\theta}_1 Y_1 + \underline{\theta}_2 Y_2 + Y_3\,,\\
B_{\delta_s,1} &= B_{\delta_s,2} = \frac{\pi}{180\lambda_s}\left[\begin{array}{cccc} \frac{C_{\alpha,f}J_{xeq}}{mJ_{xx}}\overline{\theta}_1 & \frac{C_{\alpha,f}a}{J_{zz}} & \frac{hC_{\alpha,f}}{J_{xx}} & 0 \end{array}\right]^T,\\
B_{\delta_s,3} &= B_{\delta_s,4} = \frac{\pi}{180\lambda_s}\left[\begin{array}{cccc} \frac{C_{\alpha,f}J_{xeq}}{mJ_{xx}}\underline{\theta}_1 & \frac{C_{\alpha,f}a}{J_{zz}} & \frac{hC_{\alpha,f}}{J_{xx}} & 0 \end{array}\right]^T,
\end{aligned}$$

where

$$Y_1 = \left[\begin{array}{cccc} -\frac{\sigma J_{xeq}}{mJ_{xx}} & 0 & -\frac{hc}{J_{xx}} & \frac{h(mgh-k)}{J_{xx}} \\ 0 & -\frac{\kappa}{J_{zz}} & 0 & 0 \\ 0 & \frac{h\rho}{J_{xx}} & 0 & 0 \\ 0 & 0 & 0 & 0 \end{array}\right],$$

$$Y_2 = \left[\begin{array}{cccc} 0 & \frac{\rho J_{xeq}}{mJ_{xx}} & 0 & 0 \\ 0 & 0 & 0 & 0 \\ 0 & 0 & 0 & 0 \\ 0 & 0 & 0 & 0 \end{array}\right],$$

$$Y_3 = \left[\begin{array}{cccc} 0 & -1 & 0 & 0 \\ \frac{\rho}{J_{zz}} & 0 & 0 & 0 \\ -\frac{h\sigma}{J_{xx}} & 0 & -\frac{c}{J_{xx}} & \frac{mgh-k}{J_{xx}} \\ 0 & 0 & 1 & 0 \end{array}\right].$$

We used Theorem 1 to design a controller which guarantees performance levels γ_1 and $\gamma_2 = mg\gamma_1$, in presence of the any variations in speed satisfying $\underline{v} \le v \le \overline{v}$. We achieved $\gamma_1 = 0.0097$. Also the corresponding control gain matrix is

$$K_{robust} = mg \cdot \left[\begin{array}{cccc} -14.8499 & 5.4573 & 0.1372 & -4.6320 \end{array}\right].$$

Note that, according to (22) the maximum theoretical driver steering disturbance input permitted is, $\delta_{s,\max} = 1/\gamma_1 \approx 102.60^\circ$. In our simulations however, for the reasons explained in Remark 2, the robust controller was able to keep $|LTR_d| \le 1$ for driver steering inputs with magnitudes up to $\delta_{s,\max} = 165^\circ$.

For numerical simulations, we used the same obstacle avoidance ('elk-test') scenario as before (see Figure 6), however with a peak driver steering input of magnitude $\delta_{s,\max} = 102.60^\circ$ and an initial speed of $v = 40m/s$. Comparison of the LTR_d response with with a steering input of $\delta_{s,\max} = 102.60$deg in Figure 12 shows that both controllers result in similar LTR_d responses. However inclusion of the vehicle speed as a varying parameter uncertainty in the controller design does not improve the rollover prevention capability of the vehicle.

The steering profile corresponding to this maneuver and a comparison of speed histories for the uncontrolled vehicle as well as the controlled vehicles with the two suggested control designs are shown in Figure 13. Both controllers show similar control histories and deceleration profiles, with the fixed velocity controller ending with a final velocity of 6.98m/s and the robust controller with 7.07m/s.

It is of particular interest for us to see how the suggested controllers affect the vehicle path, shown in Figure 14. The trajectory of the vehicle CG with and without controllers shows where the rollover for the uncontrolled vehicle occurs and a comparison of the response from both controllers relative to the uncontrolled case. The fixed velocity controller shows a tighter turn radius than the robust controller through the initial steering input, resulting in a slightly higher lateral translation of 20.1m to the robust controller's 19.9m from the initial lateral position. Also, because of the changing velocities and effects of tire force saturation, the symmetric input as shown in Figure 6 does not result in the vehicle heading returning to its initial direction. However in a real driving situation a driver would be able to react to the difference in heading and control the steering wheel such that the final trajectory was purely longitudinal if necessary. Furthermore, the yaw angles (measured inertially) at each longitudinal position for each controller is shown below to illustrate that the vehicle does maintain the correct orientation throughout the trajectory (i.e. the vehicle does not spin out at any point in the maneuver).

Comment : From the simulation results for the fixed model and the robust controllers, we observe that both controllers are effective in reducing the vehicle load transfer ratio LTR_d, and thus preventing rollover, however no notable improvement is achieved using the 'robust' controller.

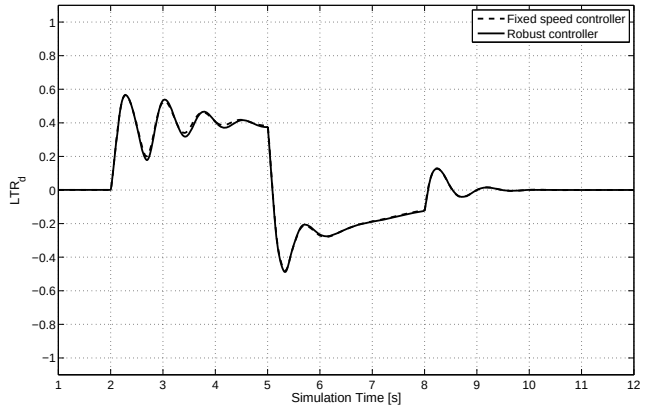

Figure 12: LTR_d response for comparison for different controllers K_{uconst} and K_{robust}

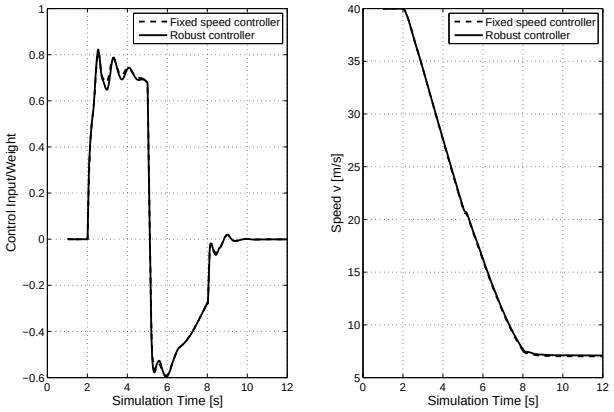

Figure 13: Comparison of control histories and longitudinal velocities for both controllers

Comment : Our design is easily extended to incorporate other sources of parameter uncertainty such as the vehicle parameters, mass and center of gravity height.

Since the wheel can only deliver as much lateral and braking force as the friction circle permits, it is of interest to compare the commanded braking force and the actual braking force on each tire; this is shown in Figure 15. Both the fixed speed and robust controllers have near identical control input histories and responses, so although the values shown in Figure 15 apply to the robust controller, there is little deviation if plotted using simulation data corresponding to the fixed speed controller. The commanded braking force from the differential braking controller ('Cmd'), the actual braking force applied to the tire ('Act') and the maximum available braking force as determined by the vertical load and the ground friction coefficient ('Avail') for each wheel is shown for the maneuver. With the way the tire model is set up, at no point is the actual applied braking force ('Act') allowed to exceed the maximum available force ('Avail'), however between t=2s and t=5s on the right rear tire the commanded braking force far exceeds the available force and thus the braking force saturates. Similarly when the steering input switches directions at $t = 5$ s, it can be seen that the commanded braking force on the rear left tire exceeds the available force.

Due to the friction circle constraint, if most of the available friction force on a tire is being used to apply a braking effort then there is little lateral force acting on that tire and load transfer is reduced. Of course, this reduces lateral acceleration and the vehicle effectively slides out of the initiated turn. The above remarks suggest that that the controller can be designed for better performance if longitudinal load transfer is taken into consideration.

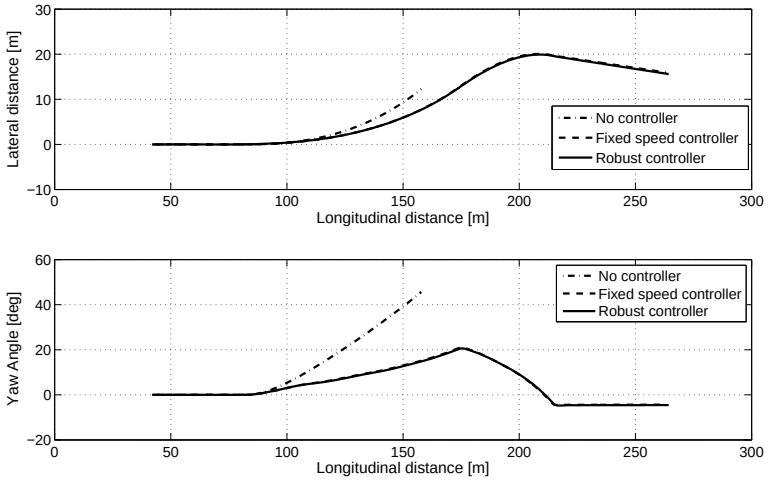

Figure 14: Comparison of CG trajectories and yaw angles

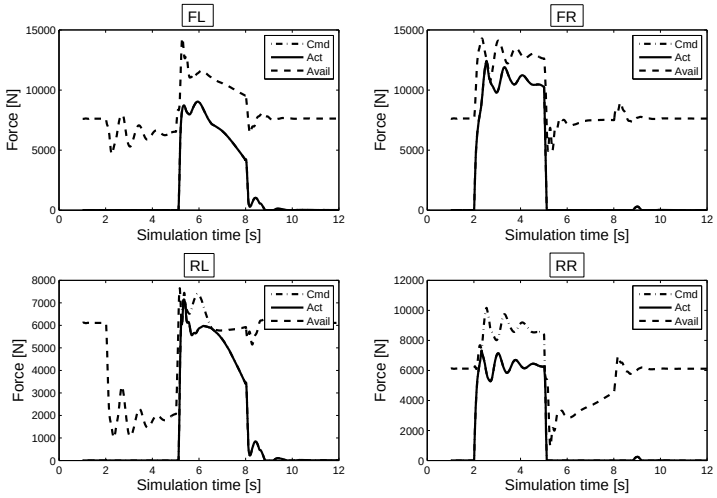

Figure 15: Commanded and actuated braking forces of each wheel

6 Conclusions

We have presented a methodology for the design of vehicle rollover prevention systems using differential braking. By introducing the load transfer ratio LTR_d, we obtain a system performance output whose value provides an accurate measure for determining the onset of rollover. Our rollover prevention system is based upon recent results from Pancake, Corless and Brockman, which provide controllers to robustly guarantee that the peak values of the performance outputs of an uncertain system do not exceed certain values. Simulation of the differential braking controller on a high-fidelity nonlinear vehicle model demonstrates the benefits of the proposed approach in a real-life problem.

References

[1] National Highway Traffic Safety Administration (NHTSA), *Traffic Safety Facts 2004: A Compilation of Motor Vehicle Crash Data from the Fatality Analysis Reporting System and the General Estimates System*, Technical Report, 2006.

[2] Runge, J., *Statement to the Committee on Commerce on SUV Safety,* 2003, (available at http://www.nhtsa.dot.gov.)

[3] Chou, C.C., McCoy, R.W. and Le, J., "A literature review of rollover test methodologies," *Int. J. Vehicle Safety,* Vol. 1, pp. 200-237, 2005.

[4] Chou, C.C., Wu, F., Gu, L. and Wu, S.R., "A review of mathematical models for rollover simulations," *AMD-Vol. 230/BED-Vol. 41, Crashworthiness, Occupant Protection and Biomechanics in Transportation Systems,* ASME, 1998.

[5] Carlson C.R. and Gerdes J.C., "Optimal rollover prevention with steer by wire and differential braking", *Proceedings of the ASME International Mechanical Engineering Congress and Exposition, IMECE'03,* Washington, D.C., USA, 2003.

[6] Pancake T., Corless M. and Brockman M., "Analysis and control of polytopic uncertain/nonlinear systems in the presence of bounded disturbance inputs", *Proceedings of the American Control Conference*, Chicago, IL, USA, 2000.

[7] Pancake T., Corless M. and Brockman M., "Analysis and Control of a class of uncertain/nonlinear systems in the presence of bounded disturbance inputs", in preparation.

[8] Palkovics L., Semsey À. and Gerum E., "Roll-over prevention system for commercial vehicles-additional sensorless function of the electronic brake system", *Vehicle System Dynamics*, Vol. 4, pp. 285-297, 1999.

[9] Wielenga T.J., "A method for reducing on-road rollovers: anti-rollover braking", *SAE Paper* No. 1999-01-0123, 1999.

[10] Chen B. and Peng H., "Differential-braking-based rollover prevention for sport utility vehicles with human-in-the-loop evaluations", *Vehicle System Dynamics*, Vol. 36, pp. 359-389, 2001.

[11] Ackermann J. and Odenthal D., "Robust steering control for active rollover avoidance of vehicles with elevated center of gravity", *Proceedings of International Conference on Advances in Vehicle Control and Safety*, Amiens, France, 1998.

[12] Odenthal D., Bünte T. and Ackermann J., "Nonlinear steering and braking control for vehicle rollover avoidance", *Proceedings of European Control Conference*, Karlsruhe, Germany, 1999.

[13] Kiencke U. and Nielsen L., *Automotive Control Systems for Engine, Driveline and Vehicle,* Springer-Verlag & SAE Int., Berlin, 2000.

[14] Kamnik R., Böttiger F. and Hunt K., "Roll dynamics and lateral load transfer estimation in articulated heavy freight vehicles: A simulation study", *Proceedings of the Institution of Mechanical Engineers*, Part D, 2003.

[15] Shorten R., Solmaz S. and Akar M., Method for determining the centre of gravity for an automotive vehicle, US Patent no: US 2009/0024269 A1, Publication date: January 22, 2009.

[16] Pacejka, H.B., *Tire and Vehicle Dynamics, Second Edition*, SAE Int., 2006

[17] Chiu, J., "A Simulink Model For Vehicle Rollover Prediction and Prevention", MS Thesis, Purdue University, 2008.

[18] Schofield, B., "Vehicle Dynamics Control for Rollover Prevention", Licentiate Thesis, Lund University, 2006.

[19] Sugiyama, H., Shabana, A., Omar, M. and Loh, W., "Development of nonlinear elastic leaf spring model for multibody vehicle systems", *Computer Methods in Applied Mechanics and Engineering*, Vol. 195 No. 50-51, pp. 6925-6941, 2006.

[20] Solmaz S., Corless M. and Shorten R., "A methodology for the design of robust rollover prevention controllers for automotive vehicles: Part 2-Active steering", HYCON-CEMaCS Joint Workshop on Automotive Systems & Control, June 1-2, 2006.

[21] Solmaz S., Corless M. and Shorten R., "A methodology for the design of robust rollover prevention controllers for automotive vehicles with active steering", *International Journal of Control*, Vol. 80, No. 11, pp. 1763-1779, November 2007.

[22] Schofield, B., Hägglund, T., and Rantzer, A., "Vehicle Dynamics Control And Controller Allocation for Rollover Prevention", *Proceedings of the IEEE International Conference on Control Applications*, Munich, Germany, 2006.

[23] Schofield, B., and Hägglund, T., "Optimal Control Allocation in Vehicle Dynamics Control for Rollover Mitigation", *Proceedings of the 2008 American Control Conference*, Seattle, WA, USA, 2008.